

# Multi-decadal warming of Atlantic water and associated decline of dissolved oxygen in a deep fjord

Dag L. Aksnes<sup>a,\*</sup>, Jan Aure<sup>b</sup>, Per-Otto Johansen<sup>c</sup>, Geir Helge Johnsen<sup>d</sup>, Anne Gro Veia Salvanes<sup>a</sup>

<sup>a</sup> Department of Biosciences, University of Bergen, Bergen, Norway

<sup>b</sup> Institute of Marine Research, Bergen, Norway

<sup>c</sup> Uni Research, Bergen, Norway

<sup>d</sup> Rådgivende Biologer, Bergen, Norway

## ARTICLE INFO

### Keywords:

Ocean warming  
Density stratification  
Oxygen decline  
Mesopelagic  
fjords

## ABSTRACT

Previous studies have shown decline in dissolved oxygen of the ocean basins. A hypothesis for this development is that ocean warming through increased stratification has caused reduced ventilation of the interior ocean. Here we provide evidence that reduced ventilation, which has been associated with a 1 °C warming of the North Atlantic Water (NAW), has contributed to recent deoxygenation of the mesopelagic zone of a Norwegian fjord, Masfjorden. Our results suggest that after the North Atlantic “Great Salinity Anomalies” around 1980, this warming has led to a decreased frequency of high-density intrusions of oxygen rich NAW and thereby reduced the renewal of the basin water of Masfjorden. From this, we infer that the basin water of other deep fjords are prone to similar development and briefly discuss some potential implications of deoxygenation in the mesopelagic zone.

## 1. Introduction

Ocean warming and deoxygenation have become a large concern worldwide (Diaz and Rosenberg, 2008; Keeling et al., 2010; Breitburg et al., 2018; Levin, 2018). The open ocean, but also coastal waters, have lost oxygen over the past 50 years (Gilbert et al., 2010; Schmidtko et al., 2017; Oschlies et al., 2017), in particular along continental margins and enclosed seas (Diaz and Rosenberg, 2008; Gilly et al., 2013; Breitburg et al., 2018). Oxygen declines in estuaries, coastal bays and marginal seas (e.g. the Baltic Sea) are often linked to discharges of sewage and agricultural fertilizer runoff leading to eutrophication (Breitburg et al., 2018; Kemp et al., 2005; Rabalais, 2002). Reduced ventilation related to warming and increased density stratification are likely a major cause for deoxygenation of the ocean interior (Schmidtko et al., 2017; Breitburg et al., 2018). Here, we hypothesize that this mechanism also affects the interior of deep fjords. The Norwegian coastline embeds more than 1 000 fjords with a maximal depth of 1 308 m (Sognefjorden). Other countries with numerous fjords are Scotland, Canada, Chile, Argentina, and New Zealand. The Norwegian fjords are commonly long, narrow, and deep inlets carved out by glaciers and filled with seawater after the last glacial maximum around 17 000 years ago (Syvitski et al., 1987). At the fjord entrance there is often a topographical barrier, the sill, which separates the fjord basin from the

ocean (Fig. 1). The fjord basin refers to the fjord volume situated deeper than the sill depth. The frequency and extent of basin water renewal, and thereby supply of new dissolved oxygen, depend on the sill depth as the sill hinders direct horizontal communication between the basin water and the oceanic water (Syvitski et al., 1987). In periods with no or minor basin water renewal, microbial oxygen consumption causes oxygen decline and the basin may turn into hypoxia and anoxia. The residence time of the basin water depends on three factors (Stigebrandt, 2012): The spectral distribution of the temporal density fluctuations of the water just above the sill depth outside the fjord, the rate of the density reduction of the basin water due to diapycnal mixing, and the time it takes to fill the basin with new water. For many fjords, this time scale is long relative to the time scale for density variations and numerous partial exchanges might take place. For such fjords, as with the interior ocean, we expect that increased warming induced stratification should reduce the DO ventilation of fjord basins. Here, we investigate the hypothesis that recent warming of the North Atlantic Water (NAW), through seawater density reduction, has contributed to reduced ventilation and oxygen decline in Norwegian fjord basins.

\* Corresponding author. University of Bergen, Department of Biosciences, Thormøhlensgate 53A/B, 5006, Bergen, Norway.  
E-mail address: [dag.aksnes@uib.no](mailto:dag.aksnes@uib.no) (D.L. Aksnes).

<https://doi.org/10.1016/j.ecss.2019.106392>

Received 25 April 2019; Received in revised form 26 August 2019; Accepted 16 September 2019

Available online 17 September 2019

0272-7714/ © 2019 The Authors. Published by Elsevier Ltd. This is an open access article under the CC BY license (<http://creativecommons.org/licenses/by/4.0/>).

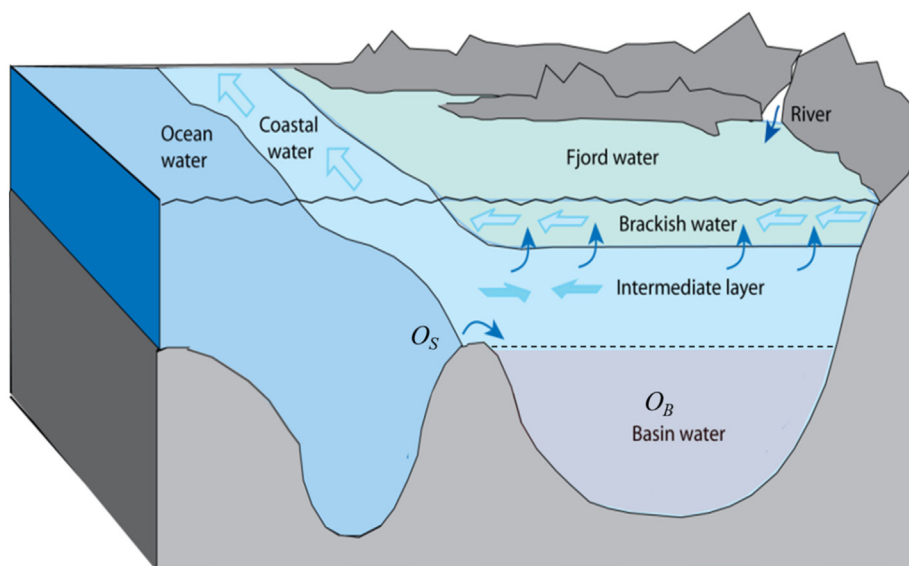


**Fig. 1.** The three vertical layers of a Norwegian fjord (not drawn to scale). At the top is a thin brackish layer (less than a few meters). Below is the intermediate layer, which extends down to the sill depth. This layer contains coastal water (Norwegian Coastal Water, NCW). If the sill is sufficiently deep, the intermediate layer also contains oceanic water (North Atlantic Water, NAW) below a layer of NCW. Under the intermediate layer is the basin water, which depending on the sill depth, contains NCW or NAW or a mixture of the two.  $O_B$  and  $O_S$  refer to the dissolved oxygen concentration in the basin water and in the oceanic source water respectively. During basin ventilation, the source water supplies new oxygen to the fjord basin. Modified after (Sætre, 2007).

## 2. Methods

### 2.1. General fjord characteristics

Fjords generally have three distinct layers. A brackish layer formed by fresh water supplies from the local watershed makes up the first layer (Fig. 1). The thickness of this layer is commonly 1–5 m depending on the magnitude of the fresh water supplies relative to the size of the fjord. Fjords are often categorized as estuaries, but estuarine circulation is generally a minor feature compared to the circulation in the intermediate layer (Stigebrandt, 2012), which is also the case for the fjord addressed in this study, Masfjorden (Aksnes et al., 1989). The intermediate layer sits between the brackish layer and the depth that corresponds to the depth of the sill (Fig. 1). The sill depth varies from a few meters (small and shallow fjords termed polls) to several hundred meters for large and deep fjords. For Masfjorden the sill depth is 70 m. The intermediate water has largely the same properties as the water at corresponding depths outside the fjord. The Norwegian Coastal Current (Figs. 1 and 2) and the wind patterns along the Norwegian coast affect the circulation in this layer (Aksnes et al., 1989; Sætre, 2007). Between the sill depth and the maximal bottom depth of the fjord, we find the basin water (Fig. 1). Three main processes control the basin water DO

concentration in fjords where the sill depth is deeper than the euphotic zone (Aure and Stigebrandt, 1989; Aksnes and Lie, 1990); Oxygen consumption due to biological activity, vertical turbulent diffusivity, and basin water renewals caused by intrusions of water with density that exceeds the basin water density. Below, we refer to such intrusions as high-density intrusions. The water masses of such intrusions originate at depths outside the fjord, which correspond to the sill depth, because they need to pass above the sill depth (i.e. in the intermediate layer) in order to intrude into the fjord basin.

### 2.2. Basin water observations in Masfjorden

The Masfjorden fjord basin extends from 70 m, which is the sill depth of the fjord, down to the maximal bottom depth of 489 m (60°52.3'N, 5°24.7'E, Fig. 2). Measurements from this deepest location have been obtained once a year, although with some missing years, in the period from 1975 to 2017 by research vessels from the University of Bergen or the Institute of Marine Research in Bergen. Prior to 1987, observations were obtained with Nansen Ocean Sampling Bottles equipped with reversing thermometers. The vertical resolution was 100 m and we report water temperature, salinity, and dissolved oxygen as a non-weighted arithmetic average of the measurements taken at

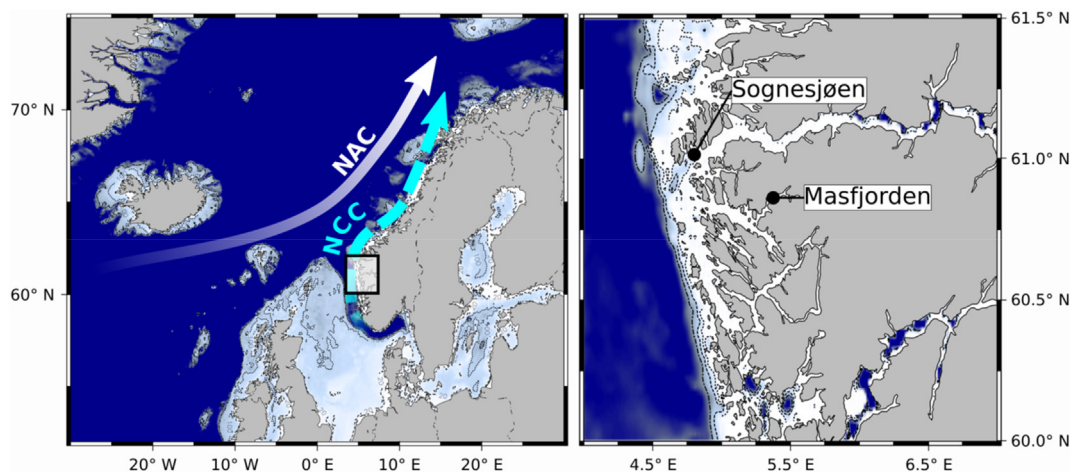


**Fig. 2.** Location of Masfjorden and the permanent hydrographical station, Sognesjøen, which has been operated since 1935. The North Atlantic Current (NAC) is a northern branch of the Gulf Stream that transports North Atlantic Water (NAW, salinity > 35) into the Norwegian Sea, and the Norwegian Coastal Current (NCC) forms a wedge of less saline Norwegian Coastal Water (NCW, salinity < 34.5) along the Norwegian coast.

200, 300, and 400 m depth. Salinity was determined with a laboratory inductivity salinometer and temperature and salinity were calibrated according to standardized procedures. DO concentration was determined by the standard Winkler technique. From 1987, temperature and salinity were measured using CTD systems mounted on the research vessels (RV Håkon Mosby and RV G.O. Sars) while DO content was determined in water samples using the Winkler technique or with a calibrated oxygen sensor attached to the CTD system.

### 2.3. Observations at Sognesjøen hydrographical station

Institute of Marine Research in Bergen has monitored salinity and temperature at Sognesjøen (Fig. 2) each second week since 1935 and observations are continuously being updated and available at: <http://www.imr.no/forskning/forskningsdata/stasjoner/view?station=Sognesjoen>. This station along with another seven stations along the Norwegian coast, which are still operated today, were set up to monitor the hydrographical properties in the Norwegian Coastal Current (NCC, Fig. 2). The NCC contains the fresher and less dense NCW that flows above the NAW originating from the North Atlantic Current. Prior to 1992, salinity and temperature were measured by use of Nansen Ocean Sampling Bottles with reversing thermometers, while a CTD system has been used afterwards. CTD measurements have been calibrated by use of reversing thermometer and collection of a water sample at the deepest depth of the CTD cast. We determined sigma-t from salinity and temperature according to UNESCO (1983).

### 2.4. Calculations of oxygen ventilation rate and a proxy for the likelihood of basin water renewal

We estimated oxygen ventilation rates from the annual changes in DO concentrations of the Masfjorden basin. We also calculated the annual frequency of high-density events (HD-frequency) from the time-series of seawater density at the Sognesjøen hydrographical station. The Sognesjøen HD-frequency serves as a proxy for the likelihood of high-density intrusions and the associated water renewal of the Masfjorden basin. Then, we used regression analysis to test to what extent the Sognesjøen HD-frequency could account for the annual variations in the oxygen ventilation rates of the Masfjorden basin.

#### 2.4.1. Estimation of the oxygen ventilation rate of the Masfjorden basin

As noted above, oxygen consumption due to biological activity, vertical turbulent diffusivity, and basin water renewals control the basin water DO concentration in fjords where sill depth is deeper than the euphotic zone (Aure and Stigebrandt, 1989). During stagnation periods, i.e. periods without high-density intrusions of water into the basin, basin water DO concentration is controlled by biological consumption and vertical turbulent diffusion of oxygen through the boundary between the basin and the intermediate layer (Fig. 1). For deep fjord basins, like Masfjorden, the effect of turbulent diffusion through this boundary is minor compared to the total biological consumption of the basin (Aure and Stigebrandt, 1989). We approximated the oxygen ventilation rate by use of a simple model for the temporal change in basin oxygen concentration ( $O_B$ , ml l<sup>-1</sup>):

$$\frac{dO_B}{dt} = V(O_S - O_B) - b \quad (1)$$

where  $t$  is time (yr).  $O_S$  (ml l<sup>-1</sup>) is the DO concentration of the water that intrudes into the basin, i.e. of the oceanic source water (see Fig. 2), and  $V$  (yr<sup>-1</sup>) is the DO ventilation rate of the basin, which is determined by the intrusions of oceanic source water rich in DO. The rate  $b$  (ml O<sub>2</sub> l<sup>-1</sup> yr<sup>-1</sup>) reflects microbial DO consumption of the basin and DO supply by turbulent diffusion, but where DO supply by turbulent diffusion is minor compared to the consumption.

Our observations from Masfjorden contain several periods when the basin water density dropped several successive years (see Results). Such

drop in density is indicative for absence of high-density intrusions that brings new oxygen to the basin water. By assuming  $V \approx 0$  in these periods, we obtained (according to Eq. (1)) estimates of the annual oxygen consumption rate,  $b$ , from the observed decline in  $O_B$  during these periods.

Unfortunately, DO has not been measured at Sognesjøen and oxygen concentration of the source water ( $O_S$ ) was set according to observations of NAW in Fensfjorden, the fjord outside Masfjorden that have direct connection with oceanic water, in the period 1975–2005 (Sætre et al., 2010). These observations were all above 5.4 ml l<sup>-1</sup>, and we have assumed constant  $O_S$  (5.4 ml l<sup>-1</sup>) throughout the period 1975–2017.

We estimated the ventilation rate,  $V$  (yr<sup>-1</sup>), of a particular year by the use of the discrete version of Eq. (1):

$$O_{B,n} = O_{B,n-1} + [V_n(O_S - O_{B,n-1}) - b]\Delta t \quad (2)$$

where  $n$  is a particular year and  $\Delta t = 1$  yr. Rearrangement provides:

$$V_n = \frac{O_{B,n} - O_{B,n-1} + b\Delta t}{(O_S - O_{B,n-1})\Delta t} \quad (3)$$

Insertion of the  $O_B$  values for two consecutive years and the values for  $O_S$  and  $b$  (see above) provided estimates of the annual ventilation rate,  $V_n$ .

#### 2.4.2. HD-frequency at the Sognesjøen hydrographical station

Following a previous study (Aksnes et al., 2009), we derived a proxy for the likelihood of renewal of the Masfjorden basin water for the period 1935 to 2017 based on the observations (each second week) of seawater density at 75 m from the Sognesjøen hydrographical station (Fig. 2). This depth is close to the sill depth (70 m) of Masfjorden. If the seawater density observed at 75 m at Sognesjøen is lower than that of the Masfjorden basin, we expect low or no renewal of the basin water. On the other hand, if the seawater density at Sognesjøen is higher than that of the Masfjorden basin, we expect renewal of the basin water. We defined the Sognesjøen HD-frequency for a particular year as follows: The percentage of the total number of observations sigma-t exceeded 27.25 at 75 m depth at Sognesjøen that year. A sigma-t of 27.25 corresponds to the lower range of the sigma-t values observed in the Masfjorden basin (see Results).

### 2.5. Simulations

We applied Eq. (2) to simulate the DO-development of the Masfjorden basin in the period 1976–2017 by using the observed DO-concentration in 1975 as initial value. Two more simulations were included. The first was to examine if an oxygen consumption term associated with the fish farming activity in Masfjorden could account for part of the variation in the observed basin water DO, i.e. we added a term,  $b_F F$ :

$$\frac{dO_B}{dt} = V(O_S - O_B) - b - b_F F \quad (4)$$

where  $F$  is the production of fish (Gg yr<sup>-1</sup>) and  $b_F$  (ml O<sub>2</sub> l<sup>-1</sup> Gg<sup>-1</sup>) is a coefficient. This term reflects the DO consumption associated with the microbial decomposition of sinking faeces and feed materials into the basin water. We collected data on annual fish (salmon) production,  $F$ , from the five fish farms located in Masfjorden. Before 2001, the annual production was less than 0.3 Gg (1 Gg corresponds to 1 000 metric tons). After 2001, the annual production was between 0.7 and 3.8 Gg and with the most extensive farming from 2013 to 2016.

In the last simulation, we applied the model to calculate the DO-development for a period (1935–1975), for which we had density observations at the Sognesjøen station, but before we had DO observations from Masfjorden.

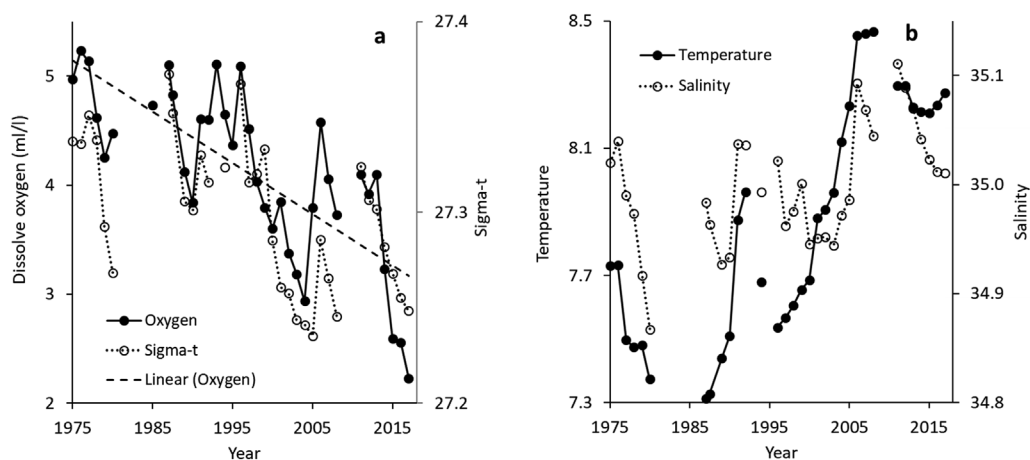


**Fig. 3.** Development in (a) dissolved oxygen (DO), sigma-t, (b) temperature ( $^{\circ}\text{C}$ ), and salinity in the basin water of Masfjorden. Observations are the average of measurements taken at 200, 300, and 400 m depth in October or November. A regression analysis (broken line,  $R^2 = 0.56$ ) indicate a multi-decadal decline in DO corresponding to  $0.047 \pm 0.014 \text{ ml l}^{-1} \text{ yr}^{-1}$  (95% c.i.,  $p < 10^{-6}$ ,  $n = 35$ ).

### 3. Results

#### 3.1. Multi-decadal decline in dissolved oxygen in the Masfjorden basin

We observed a decreasing trend ( $0.047 \pm 0.014 \text{ ml l}^{-1} \text{ yr}^{-1}$ ,  $p < 10^{-6}$ ,  $n = 35$ , Fig. 3a) in the DO concentration of the Masfjorden basin water in the period 1975–2017. This multidecadal decline corresponds to  $2.0 \text{ ml l}^{-1}$  over 42 years and concurred with an overall decline in basin water density (Fig. 3a) and associated  $1^{\circ}\text{C}$  rise in temperature (Fig. 3b). The basin salinity was on the range 34.85–35.1 with an average of 35.0 (Fig. 3b), commonly defined as NAW.

Pronounced drop in the DO concentration for several successive years is indicative of a period with low renewal of the basin, which result in stagnant basin water. In such periods, DO drops because the biological consumption is higher than the supply of new oxygen. In five such three-year periods, the DO concentration of the Masfjorden basin dropped at rates from 0.42 to  $0.75 \text{ ml O}_2 \text{ l}^{-1} \text{ yr}^{-1}$  with an average of  $0.52 \text{ ml O}_2 \text{ l}^{-1} \text{ yr}^{-1}$  (Table 1). This suggests a time scale of 7–12 years for the Masfjorden basin to turn anoxic in prolonged stagnant periods.

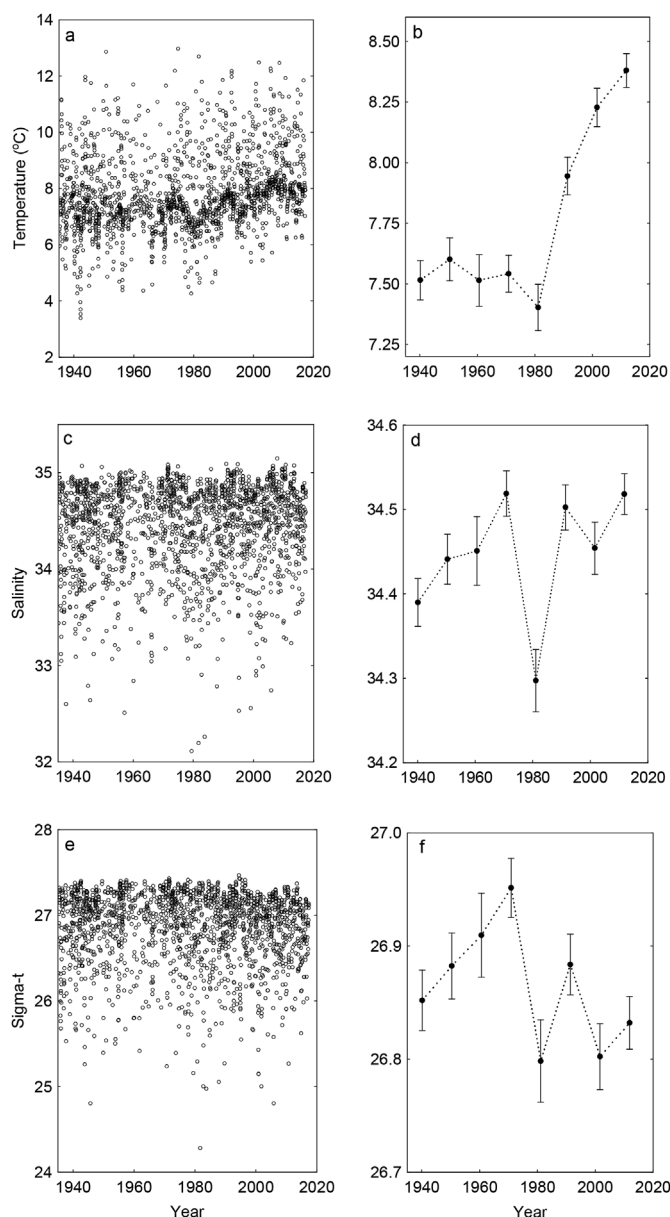
#### 3.2. Warming and associated decrease in seawater density at Sognesjøen

Fig. 4 shows the temperature, salinity, and density variations in the potential source water for the Masfjorden basin, i.e. at 75 m depth at the Sognesjøen hydrographical station. According to seasonal variations, the temperature fluctuates between 3 and  $13^{\circ}\text{C}$  (Fig. 4a). In the period from 1935 to 1970, there is no trend in the decadal temperature averages (Fig. 4b) while salinity (Fig. 4d) and density (Fig. 4f) increased. Relatively large drops in the decadal means of density and salinity (and to a smaller extent in temperature) are seen in 1980, likely associated with the Great Salinity Anomalies of the 1970's and 1980's (Belkin et al., 1998). In 1990, the decadal salinity average returns to a high level and remain high for the next decades. The density, however, did not return to the high 1970-level due to a rise in temperature. Continued increase in temperature in 2000 and 2010, and relatively small changes in salinity, ensured low density-levels in 2000 and 2010,

**Table 1**

Decline in dissolved oxygen in Masfjorden in periods with sustained drop in density. These periods were presumably stagnation periods were the oxygen decline primarily reflected biological consumption (see text).

Periods	Change in oxygen ( $\text{ml O}_2 \text{ l}^{-1} \text{ yr}^{-1}$ )	Annual change in sigma-t
1977–1979	−0.44	−0.029
1987–1989	−0.48	−0.033
1996–1998	−0.53	−0.024
2006–2008	−0.42	−0.020
2013–2015	−0.75	−0.017



**Fig. 4.** (a) Temperature, (c) salinity, and (e) density observations (each second week) and (b, d, and f) decadal averages of the same properties in the period 1935–2017 at 75 m depth at the Sognesjøen hydrographical station.

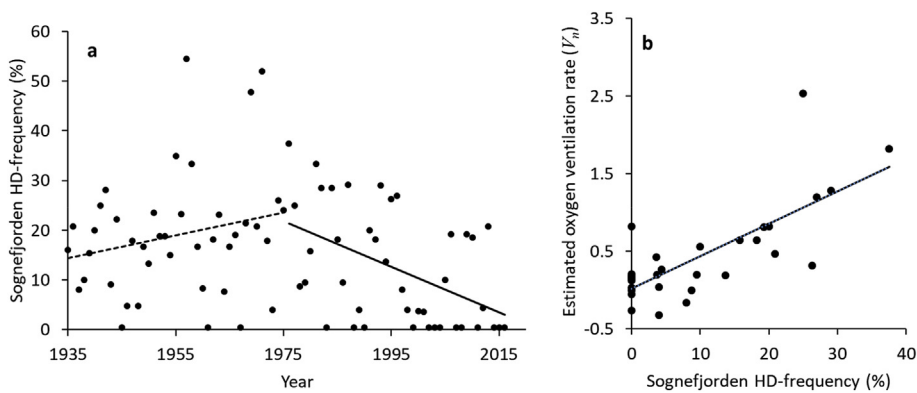


**Fig. 5.** (a) The Sognefjorden high-density frequency (HD-frequency). The linear regression lines are for the period after 1975 (solid line, decrease is  $0.47\% \pm 0.13\%$  per year,  $p < 10^{-3}$ ,  $n = 43$ ) and before 1975 (broken line,  $p = 0.16$ ). (b) The relationship between the calculated oxygen ventilation rate of the Masfjorden basin ( $V_n$  in Eqs. (2) and (3)) and the Sognefjorden HD-frequency. A regression analysis (solid line) indicates the relationship  $V_n = 0.042HD + 0.019$  ( $R = 0.75$ ,  $p < 10^{-5}$ ,  $n = 31$ ), where HD is the Sognefjorden HD-frequency.

which were similar to that observed during the low-salinity event in 1980. Thus, we identify three periods: i) From 1940 to around 1970, density increased primarily due to a gradual increase in salinity, ii) around 1980, density dropped and this drop was likely associated with the Great Salinity Anomalies, and iii) after 1990, density remained low due to increasing temperature.

After 1975, we see a trend ( $p < 0.001$ ,  $n = 43$ ) of reduced Sognefjorden HD-frequency (solid line in Fig. 5a). A HD-frequency equal to 10 means that 10% of the sigma-t observations at 75 m depth at the Sognefjorden hydrographical station exceeded 27.25 that particular year. In the late period (1975–2017), 13 years had a Sognefjorden HD-frequency of zero indicative for no high-density intrusion in the Masfjorden basin. Ten out of these occurred after 1998 when elevated temperature (Fig. 4b) gave rise to a relatively low density (Fig. 4f). The early period (1935–1975), with increasing salinity and density (Fig. 4d and f), had only three years with zero HD-frequency (Fig. 5a).

### 3.3. Oxygen ventilation of the Masfjorden basin

Fig. 5b shows the association between the estimated oxygen ventilation rate of the Masfjorden basin ( $V_n$  in Eqs. (2) and (3)) and HD-frequency at Sognefjorden after 1975. The regression analysis (solid line in Fig. 5b) indicates that the estimated oxygen ventilation rate,  $V_n$ , increases with  $0.42 \pm 0.14 \text{ yr}^{-1}$  ( $p < 10^{-5}$ ,  $n = 31$ ) when the Sognefjorden HD-frequency increases with 10 units. This association is consistent with the hypothesis that reduced density of the oceanic source water, has contributed to reduced ventilation and associated deoxygenation of the Masfjorden basin. Initially (i.e. around 1980), reduced density appears to have been associated with the Great Salinity Anomalies in the 1970's and the 1980's (Belkin et al., 1998). After the low salinity event, however, warming (Fig. 4b) appears to be the primary cause for the reduced HD-frequency and the associated deoxygenation of the Masfjorden basin.

### 3.4. Simulations of DO in the Masfjorden basin water

We used Eq. (2), which is the numerical version of Eq. (1), to simulate the DO development in the Masfjorden basin for the period 1975–2017 (Fig. 6a). The simulated development was driven by the annual oxygen ventilation rate ( $V_n$ ) that was determined by the Sognefjorden HD-frequency (see Table 2 and Fig. 5b). The two other model coefficients,  $O_b$  and  $b$ , were set constant throughout the simulated period (values in Table 2). The simulation accounted for 67% of the variation in observed DO (Fig. 6b). Another 9% of the variation in observed DO (Fig. 6c and d) was accounted for when we included the oxygen consumption term,  $b_F F$  (see Eq. (3)), which reflects the salmon farming in Masfjorden. Least square minimization provided a fish farming DO consumption rate (in the basin water),  $b_F$ , corresponding to  $0.065 \text{ ml l}^{-1}$  per 1 000 metric ton fish produced during a year (Table 2). Typical Biochemical Oxygen Demand (BOD) associated with faeces

and excess feed from Norwegian salmon farming is  $480 \times 10^6 \text{ g O}_2$  per 1 000 metric ton fish production (Bergheim and Braaten, 2007), which corresponds to  $340 \times 10^6 \text{ ml O}_2 \text{ l}^{-1}$  at a temperature of  $8^\circ\text{C}$  and salinity 35. Dividing this BOD estimate with the volume of the basin water of Masfjorden ( $3\,560 \times 10^6 \text{ m}^3$ , Aksnes et al., 1989) indicates an oxygen consumption of  $0.1 \text{ ml l}^{-1}$  per 1 000 metric ton fish produced during a year, which is of the same order as the  $b_F$  estimate.

The observations at the Sognefjorden hydrographical station goes back to 1935 and this enabled a simulation of the basin water oxygen conditions for the entire period 1935–2017 (Fig. 7). Since the DO concentrations of the Masfjorden basin prior to 1975 is unknown, an initial value had to be chosen for 1935. However, because the Sognefjorden HD-frequencies in 1935 and 1936 were high (Fig. 5a), and consequently also the estimated oxygen ventilation rates ( $V_n$ ), the DO development in successive years was insensitive to the choice of the initial DO-value (Fig. 6). According to the simulation, frequent high-density events in the oceanic source water ensured that high oxygenation ( $\text{DO} > 4 \text{ ml l}^{-1}$ ) persisted for around 50 years. The simulated development catch well up with the measured DO value in 1975 and consequently with the observations thereafter.

## 4. Discussion

Our results suggest that reduced seawater density of the oceanic source water has led to a reduction in the ventilation rate and thereby contributed to the observed multi-decadal DO decline in the Masfjorden basin. Initially, reduced salinity, which was likely associated with the Great Salinity Anomalies around 1980 (Belkin et al., 1998), caused a density reduction. After this event, warming of the oceanic source water (NAW) kept the density low despite that the salinity returned to the high 1970 level. The development after the Great Salinity Anomaly is consistent with the hypothesis that increased warming induced stratification has contributed to oxygen decline in Masfjorden. In the period 2013–2017, an improvement in the fit between simulated and observed DO-values suggests that high fish farming activity also contributed to the DO decline and illustrates how reduced basin ventilation decreases the holding capacity for fish farming. Because the ventilation mechanism of many Norwegian fjord basins is similar to that of Masfjorden, our results are likely relevant elsewhere along the Norwegian coast. This might have important societal and economic implications since the economic value of fish farming in sheltered coastal waters by far exceeds that of the total Norwegian landings of wild caught fish in the North Sea, the Norwegian Sea and the Barents Sea.

Surprisingly, there are few studies of long-term DO development in Norwegian fjord basins. Sætre et al. (2010) do report a time-series at 300 m depth in Byfjorden outside Bergen for the period 1926–2005, although with a pronounced gap between 1965 and 1980. Prior to 1965, the DO concentration was high ( $4.8\text{--}6.8 \text{ ml l}^{-1}$ ) while a decline was reported for the period 1980–2005, similar to what is indicated in our simulation of Masfjorden (Fig. 7). Johansen et al. (2018) report that

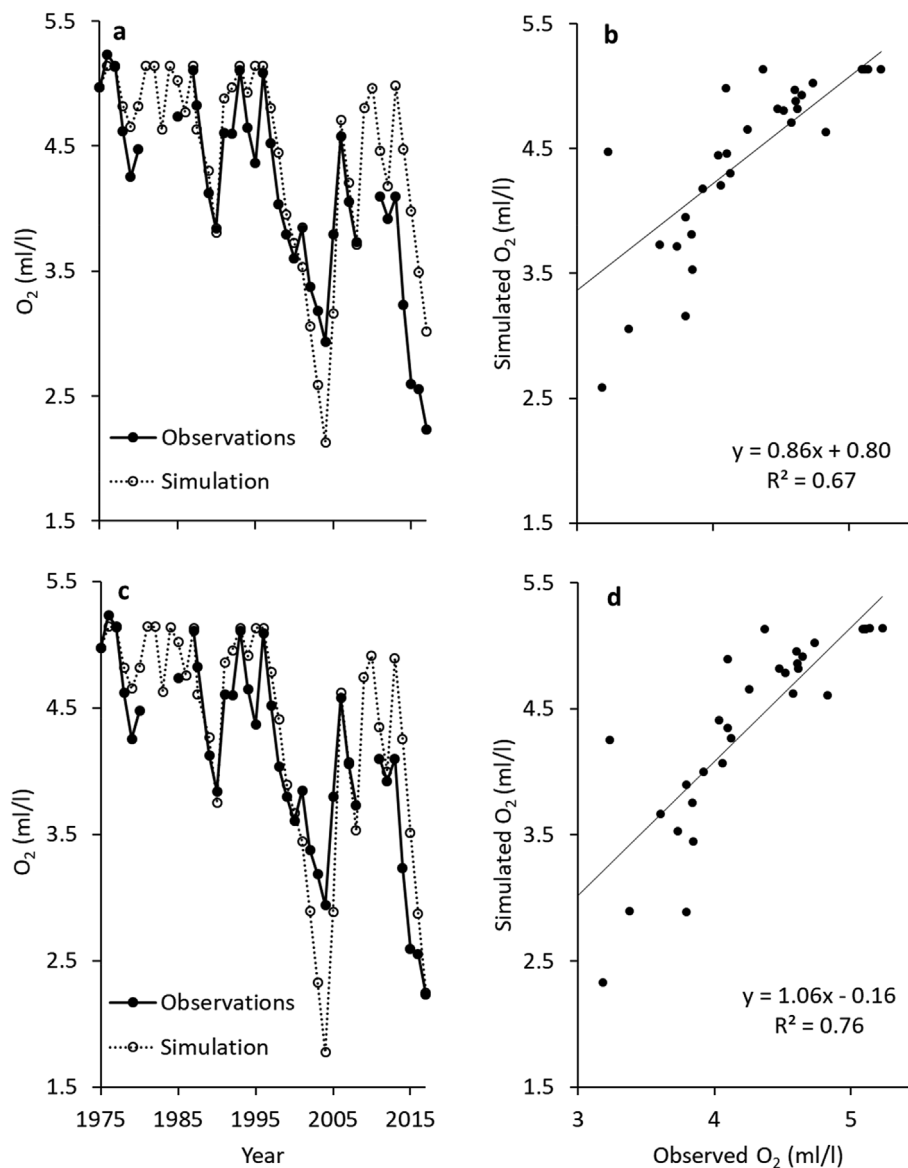


Fig. 6. The simulated (Eqs. (1) and (2)) DO in the Masfjorden basin plotted against (a) time and (b) observed DO. Values of the three model coefficients  $V_n$ ,  $O_B$  and  $b$  are shown in Table 2. The improved fit in (c) and (d) was obtained by adding a fish farm oxygen consumption coefficient ( $b_F$ , see Eq. (4)). An estimate of this coefficient (Table 2) was obtained by fitting simulated and observed DO by least squares minimization.

this decline has continued after 2005, and concurrently they found increased number of opportunistic benthic species.

Schmidtke et al. (2017) found that around 15% of the DO-decline in the global ocean is a direct effect of warming-induced decrease in DO-solubility and that reduced ventilation of the interior ocean, because of intensified stratification, may account for the remaining 85% although this is uncertain. Decreased DO-solubility may also have contributed somewhat to the multi-decadal DO decline in Masfjorden, but as for the ocean interior, our results suggest that the oxygen is particularly

sensitive to warming induced density stratification. If the NAW warming trend continues, we expect that low ventilation and DO will prevail until the warming trend ceases or reverses. Increased salinity of the source water might counteract the effect from warming, while freshening likely will strengthen the negative effect on basin ventilation.

Table 2

Values of the coefficients used in simulating time-series of basin water DO (Eqs. (1), (2) and (4)). The unit of  $b_F$  ( $\text{ml l}^{-1} \text{Gg}^{-1}$ ) corresponds to  $\text{ml l}^{-1}$  per 1000 metric ton fish production.

Coefficient	Symbol	Unit	Estimate	Source
Ventilation rate	$V_n$	$\text{yr}^{-1}$	$V_n = 0.042f + 0.019$	Fig. 5b
DO consumption rate in stagnant periods	$b$	$\text{ml l}^{-1} \text{yr}^{-1}$	0.52	Average of values in Table 1
DO in source water	$O_S$	$\text{ml l}^{-1}$	5.4	Sætre et al. (2010)
Fish farming DO consumption coefficient (Eq. (4))	$b_F$	$\text{ml l}^{-1} \text{Gg}^{-1}$	0.065	Estimated by curve fitting (Fig. 6c-d)

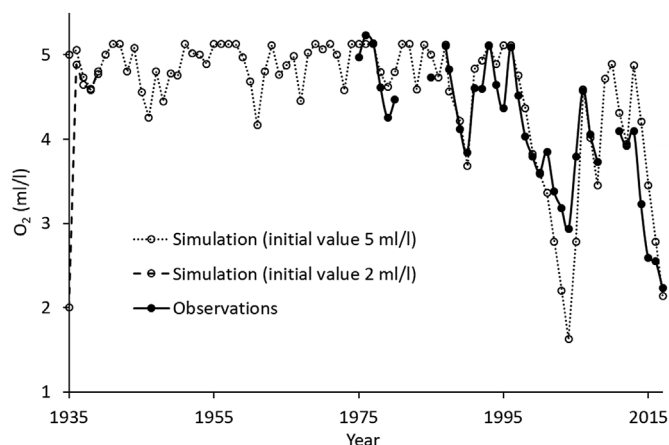


Fig. 7. Simulation of DO in the Masfjorden basin (Eq. (4)) including the period (1935–1975) prior to the DO observations (1975–2017). The values of the coefficients used in the simulation are given in Table 2. Due to high Sognesjøen HD-frequency in 1935 and 1936 (Fig. 5a), the simulated time-series was insensitive to the choice of initial DO-value in 1935. This is illustrated by the initial values of 2 and 5 ml<sup>-1</sup> which provide converging developments early on.

#### 4.1. Deoxygenation affects the mesopelagic biota

Deoxygenation of deep fjords primarily affects the mesopelagic and the associated benthic habitat. In terms of light, this part of the water column corresponds to the dysphotic zone where light intensity is insufficient for photosynthesis, but sufficient for vision in many organisms. The mesopelagic/dysphotic zone is commonly defined as the depth zone 200–1 000 m, but due to lower light transmission than in clear oceanic water, this zone is shallower in fjords (Røstad et al., 2016a, b; Kaartvedt et al., 2019). Deep fjords deviate from other coastal ecosystems like estuaries and shelf-systems in that the mesopelagic habitat is not only the largest in terms of volume, but also in terms of animal biomass due to the presence of mesopelagic fishes and invertebrates (Giske et al., 1990; Salvanes et al., 1995). In this sense, deep fjords are more similar to the open ocean where the oxygen minimum zones and their effect on the mesopelagic biota is an important feature (Bianchi et al., 2013; Irigoien et al., 2014; Klevjer et al., 2016; Koslow et al., 2011). Although mobile animals are able to escape from hypoxic environments, expansion of oxygen minimum zones leads to vertical compression of available habitat for many higher organisms (Gallo and Levin, 2016; Gilly et al., 2013; Netburn and Koslow, 2015). In a fjord study, Solberg et al. (2015) demonstrated vertical habitat compression for fish. Solitary swimming individuals were observed near bottom under moderate hypoxia, while during a year when basin water was severely hypoxic, the individuals schooled in midwater and only took short-term dives into hypoxic waters to feed on overwintering zooplankton (Solberg et al., 2015).

There is observational evidence that mesopelagic hypoxic water has elevated light attenuation (Aksnes et al., 2017; Kaartvedt et al., 2019). Furthermore, it has recently been shown (McCormick and Levin, 2017) that, due to high energy requirement of vision, visual predators such as fishes will have a disadvantage under low oxygen conditions. Thus the combined direct and indirect effect (through light attenuation) of deoxygenation on visual performance reinforces the effect oxygen depletion has on vertical shoaling and compression of the habitat. Thus in addition to the effect deoxygenation has on benthic fjord communities (Johansen et al., 2018), it is a likely driver for a visibility-initiated shift from visual to tactile predators in fjord ecosystems (Aksnes et al., 2009; Bagøien et al., 2001; Eiane et al., 1999; Sørnes et al., 2007).

## 5. Conclusion

Our analysis suggests that sustained warming of the oceanic source water has contributed to oxygen decline in Masfjorden after the Great Salinity Anomaly around 1980 (Belkin et al., 1998), but likely also in other fjord basins with long basin water residence times. In addition to negative effects on benthic and mesopelagic biodiversity, deoxygenation reduces the holding capacity for fish farming (Aure and Stigebrandt, 1990; Stigebrandt et al., 2004) with socioeconomic implications. Our study has demonstrated that the IMR coastal hydrographic stations (<http://www.imr.no/forskning/forskningsdata/stasjoner/>), which have been operated since the 1930's, are a valuable asset in monitoring the boundary conditions of Norwegian fjord basins. We think that future environmental assessment and analysis, as well as management of fish farming, will benefit greatly from an upgrade involving more frequent measurements than today (each second week) and from inclusion of measurements of dissolved oxygen.

## Declarations of interest

None.

## Acknowledgement

We thank Tom Langbehn for help with the illustrations.

## Appendix A. Supplementary data

Supplementary data to this article can be found online at <https://doi.org/10.1016/j.ecss.2019.106392>.

## References

- Aksnes, D.L., Aure, J., Kaartvedt, S., Magnesen, T., Richard, J., 1989. Significance of advection for the carrying capacities of fjord populations. *Mar. Ecol.: Prog. Ser.* 50, 263–274.
- Aksnes, D.L., Dupont, N., Staby, A., Fiksen, O., Kaartvedt, S., Aure, J., 2009. Coastal water darkening and implications for mesopelagic regime shifts in Norwegian fjords. *Mar. Ecol.: Prog. Ser.* 387, 39–49.
- Aksnes, D.L., Lie, U., 1990. A coupled physical biological pelagic model of a shallow sill fjord. *Estuar. Coast Shelf Sci.* 31, 459–486.
- Aksnes, D.L., Røstad, A., Kaartvedt, S., Martinez, U., Duarte, C.M., Irigoien, X., 2017. Light penetration structures the deep acoustic scattering layers in the global ocean. *Sci. Adv.* 3, e1602468.
- Aure, J., Stigebrandt, A., 1989. On the influence of topographic factors upon the oxygen consumption rate in sill basins of fjords. *Estuar. Coast Shelf Sci.* 28, 59–69.
- Aure, J., Stigebrandt, A., 1990. Quantitative estimates of the eutrophication effects of fish farming on fjords. *Aquaculture* 90, 135–156.
- Bagøien, E., Kaartvedt, S., Aksnes, D.L., Eiane, K., 2001. Vertical distribution and mortality of overwintering *Calanus*. *Limnol. Oceanogr.* 46, 1494–1510.
- Bergheim, A., Braaten, B., 2007. Modell for utslipp fra norske matfiskanlegg til sjø. IRIS report no. 2007/180. International Research Institute of Stavanger, pp. 35.
- Belkin, I.M., Levitus, S., Antonov, J., Malmberg, S.-A., 1998. “Great salinity Anomalies” in the North Atlantic. *Prog. Oceanogr.* 41, 1–68.
- Bianchi, D., Galbraith, E.D., Carozza, D.A., Mislan, K.A.S., Stock, C.A., 2013. Intensification of open-ocean oxygen depletion by vertically migrating animals. *Nat. Geosci.* 6, 545–548.
- Breitburg, D., et al., 2018. Declining oxygen in the global ocean and coastal waters. *Science* 359, eaam7240.
- Diaz, R.J., Rosenberg, R., 2008. Spreading dead zones and consequences for marine ecosystems. *Science* 321, 926–929.
- Eiane, K., Aksnes, D.L., Bagøien, E., Kaartvedt, S., 1999. Fish or jellies - a question of visibility? *Limnol. Oceanogr.* 44, 1352–1357.
- Gallo, N., Levin, L., 2016. Fish ecology and evolution in the world's oxygen minimum zones and implications of ocean deoxygenation. *Adv. Mar. Biol.* 74, 117–198.
- Gilbert, D., Rabalais, N., Diaz, R., Zhang, J., 2010. Evidence for greater oxygen decline rates in the coastal ocean than in the open ocean. *Biogeosciences* 7, 2283–2296.
- Gilly, W.F., Beman, J.M., Litvin, S.Y., Robison, B.H., 2013. Oceanographic and biological effects of shoaling of the oxygen minimum zone. *Ann. Rev. Marine Sci.* 5, 393–420.
- Giske, J., et al., 1990. Vertical distribution and trophic interactions of zooplankton and fish in Masfjorden, Norway. *Sarsia* 75, 65–81.
- Irigoien, X. et al., 2014. Large mesopelagic fishes biomass and trophic efficiency in the open ocean. *Nat. Commun.* 5, 3271.
- Johansen, P.-O., others, 2018. Temporal changes in benthic macrofauna on the west coast of Norway resulting from human activities. *Mar. Pollut. Bull.* 128, 483–495.

- Kaartvedt, S., Langbehn, T.J., Aksnes, D.L., 2019. Enlightening the ocean's twilight zone. ICES (Int. Council. Explor. Sea) J. Mar. Sci. <https://doi.org/10.1093/icesjms/fsz010>.
- Keeling, R.F., et al., 2010. Ocean deoxygenation in a warming world. *Annu Rev Mar Sci* 2, 199–229.
- Kemp, W.M., et al., 2005. Eutrophication of Chesapeake Bay: historical trends and ecological interactions. *Mar. Ecol.-Prog. Ser.* 303, 1–29.
- Klevjer, T.A., Irigoien, X., Røstad, A., Fraile-Nuez, E., Benítez-Barrios, V.M., Kaartvedt, S., 2016. Large scale patterns in vertical distribution and behaviour of mesopelagic scattering layers. *Sci. Rep.* 6, 19873.
- Koslow, J.A., Goericke, R., Lara-Lopez, A., Watson, W., 2011. Impact of declining intermediate-water oxygen on deepwater fishes in the California Current. *Mar. Ecol.-Prog. Ser.* 436, 207–218.
- Levin, L., 2018. Manifestation, drivers and emergence of open ocean deoxygenation. *Ann Rev Mar Sci* 10, 229–260.
- McCormick, L.R., Levin, L.A., 2017. Physiological and ecological implications of ocean deoxygenation for vision in marine organisms. *Philos. Trans. R. Soc. A Math. Phys. Eng. Sci.* 375.
- Netburn, A.N., Koslow, A.J., 2015. Dissolved oxygen as a constraint on daytime deep scattering layer depth in the southern California current ecosystem. *Deep Sea Res. Oceanogr. Res. Pap.* 104, 149–158.
- Oschlies, A., et al., 2017. Patterns of deoxygenation: sensitivity to natural and anthropogenic drivers. *Philos. Trans. R. Soc. London, Ser. A* 375, 20160325. <https://doi.org/10.1098/rsta.2016.0325>.
- Rabalais, N.N., 2002. Nitrogen in aquatic ecosystems. *AMBIO A J. Hum. Environ.* 31, 102–112.
- Røstad, A., Kaartvedt, S., Aksnes, D.L., 2016a. Erratum to “Light comfort zones of mesopelagic acoustic scattering layers in two contrasting optical environments” [*Deep-Sea Res. I* 113 (2016) 1–6]. *Deep Sea Res. Oceanogr. Res. Pap.* 114, 162–164.
- Røstad, A., Kaartvedt, S., Aksnes, D.L., 2016b. Light comfort zones of mesopelagic acoustic scattering layers in two contrasting optical environments. *Deep Sea Res. Oceanogr. Res. Pap.* 113, 1–6.
- Salvanes, A., Aksnes, D., Fosså, J., Giske, J., 1995. Simulated carrying capacities of fish in Norwegian fjords. *Fish. Oceanogr.* 4, 17–32.
- Schmidtko, S., Stramma, L., Visbeck, M., 2017. Decline in global oceanic oxygen content during the past five decades. *Nature* 542, 335–339.
- Solberg, I., Røstad, A., Kaartvedt, S., 2015. Ecology of overwintering sprat (*Sprattus sprattus*). *Prog. Oceanogr.* 138, 116–135.
- Stigebrandt, A., 2012. Hydrodynamics and circulation of fjords. In: Bengtsson, L., Herschy, R.W., Fairbridge, R.W. (Eds.), *Encyclopedia of Lakes and Reservoirs*. @ Springer Science + Business Media B.V. <https://doi.org/10.1007/978-1-4020-4410-6>.
- Stigebrandt, A., Aure, J., Ervik, A., Hansen, P.K., 2004. Regulating the local environmental impact of intensive marine fish farming: III. A model for estimation of the holding capacity in the Modelling–Ongrowing fish farm–Monitoring system. *Aquaculture* 234, 239–261.
- Syvitski, J.P., Burrell, D.C., Skei, J.M., 1987. *Fjords: Processes and Products*. Springer, New York, pp. 377pp.
- Sætre, R., 2007. *The Norwegian Coastal Current - Oceanography and Climate*. Tapir Academic Press, Trondheim, pp. 159.
- Sætre, R., Aure, J., Gade, H.G., 2010. Oseanografi og klima. In: Johannessen, P., Sætre, R., Kryvi, H., Hjelle, H. (Eds.), *Bergensfjordene - Natur Og Bruk*. Havforskningssinstituttet, Uni Research, Universitetet I Bergen, pp. 33–55 Bergen Kommune.
- Sørnes, T.A., Aksnes, D.L., Bamstedt, U., Youngbluth, M.J., 2007. Causes for mass occurrences of the jellyfish *Periphylla periphylla*: a hypothesis that involves optically conditioned retention. *J. Plankton Res.* 29, 157–167.
- UNESCO, 1983. Algorithms for Computation of Fundamental Properties of Seawater. *Unesco Technical Papers in Marine Science*. No. 44.